Failure Modes in Filled Hole GFRP Laminates for Connections Between FRP and Concrete

R. Lameiras[1], C. Gonçalves[2], I. Valente[3], J. Barros[4], M. Azenha[5]
[1]ISISE, Univ. of Minho, School of Eng., Guimarães, Portugal. rmlameiras@civil.uminho.pt
[2]ISISE, Univ. of Minho, School of Eng., Guimarães, Portugal. a51309@alunos.uminho.pt
[3]ISISE, Univ. of Minho, School of Eng., Guimarães, Portugal. isabelv@civil.uminho.pt
[4]ISISE, Univ. of Minho, School of Eng., Guimarães, Portugal. barros@civil.uminho.pt
[5]ISISE, Univ. of Minho, School of Eng., Guimarães, Portugal. miguel.azenha@civil.uminho.pt

Keywords: Laminate; Limit design; GFRP.

SUMMARY

The PERFOFRP connector consists on a perforated glass fibre reinforce polymer (GFRP) rib that is specially designed to perform the connection between thin concrete layers, which can be also useful in the context of structural rehabilitation. It stays embedded in the concrete layers, avoiding the use of complementary connecting techniques, like special gluing or bolting. This type of connection is similar to the Perfobond steel connectors proposed for steel and concrete composites structures. Perfobond shear connector failure depends on the concrete dowels load capacity, since the steel connector failure does not occur in ribs with adequate thickness. However, in the case of the PERFOFRP connectors, the load capacity can be limited by the failure of the connector itself. To achieve a better understanding on the behaviour of the GFRP connector, an experimental study, based on tests with perforated GFRP laminates submitted to pin-bearing tests, is carried out. The tests are performed with four different rectangular GFRP plates containing a circular hole of 30 mm diameter, and differing from each other in terms of stacking and amount of fibre plies. Two different geometries of specimens are studied to enhance the evaluation of two expected failure modes. Finally, the failure modes, the peak loads and the evolution of strain in the vicinity of the holes are presented and discussed.

1. INTRODUCTION

In the construction industry, there is an increasing interest on the use of FRP as replacement for the traditional materials. In previous works [1-3], the authors proposed the use of an innovative type of laminated GFRP rib shear connector (PERFOFRP connectors) specially designed to perform the connection between thin concrete layers (Figure 1a). This connector is embedded in the concrete layers, avoiding the use of additional connecting techniques, such as gluing or bolting.

The design of the PERFOFRP connector is inspired in the Perfobond connector that is used in steel and concrete composite beams, and consists on a metallic plate with a limited number of holes, welded to the steel beam and concreted inside the concrete slab. During casting, the plate openings are filled with concrete, forming dowels that provide resistance to horizontal shear and prevent vertical separation between the steel beam and the concrete slab [4, 5]. This effect is commonly referred as concrete dowel effect [6] (Figure 1b). The load capacity of a Perfobond connector results from the following parcels: the tensile strength on the concrete slab along the Perfobond alignment; the tensile strength of the transversal reinforcement bars; the shear resistance of the confined concrete that lies inside the connector's openings, and the bearing of compressed concrete positioned in front of the

Perfobond rib. The connector itself usually presents high shear resistance. Thus, the connector shear failure is unusual [5, 7].

On the other hand, the proposed PERFOFRP connector consists in a glass fibre reinforced polymer (GFRP) perforated plate, designed to be used with thin concrete layers. The concrete flows into the connector's holes, forming concrete dowels (Figure 1c) that provide shear resistance and avoid the separation between the connector and the concrete layer.

Using GFRP connectors can be an advantageous solution for the structural rehabilitation, since they can be used for adding a relatively thin layer of fibre reinforced concrete to increase the load carrying capacity and the thermal and acoustic performance of buildings deserving rehabilitation, without forming thermal bridges. These connectors can also be used for the development of high performance sandwich panels that can also be used in the context of building rehabilitation, as façade, floor or shear wall components [2].

Unlike Perfobond connectors, where the load capacity relies on the concrete dowels formed in the holes of the rib, the authors verified in previous works [1, 8] that PERFOFRP connectors' load capacity can be also limited by failure of the connector itself, depending on the material and geometrical properties of the connector and the type of concrete adopted. These studies showed that, in the case of using GFRPs with a low content of discontinuous fibres, the connection failure often occurs at the vicinity of the connectors' holes. Then, to predict the load capacity of these connectors, it is necessary to evaluate the isolated behaviour of the perforated connector.

Thus, this paper aims to complement the knowledge on the PERFOFRP connector, by performing an experimental study focused on the isolated effects of the concrete dowel on the GFRP connector. For this purpose, GFRP specimens comprising only one hole are prepared and bearing tests are carried out. Two specimens' geometries and four different GFRP laminate types are adopted to evaluate its influence on the behaviour of the connector. Load capacity and typical failure modes are presented and discussed.
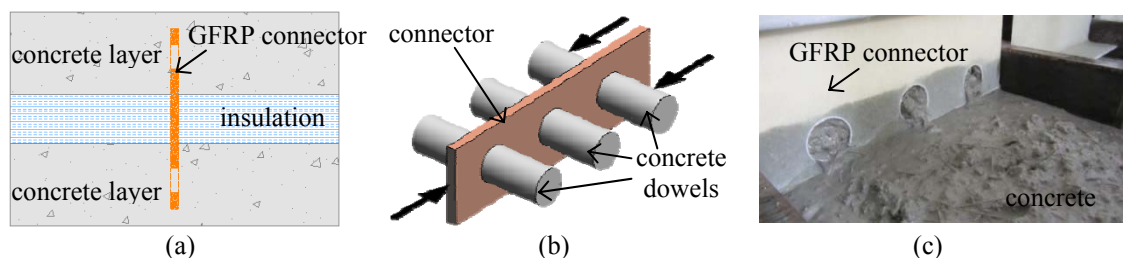

| (a) | (b) | (c) |

Figure 1: (a) Schematic view of the PERFOFRP used to join the concrete layers of a sandwich panel; (b) Concrete dowel effect [6]; (c) PERFOFRP connection during casting.

2. FABRICATION OF SPECIMENS

The laminates under investigation are produced by overlapping layers of *E* glass fabrics composed by continuous and discontinuous fibres disposed in different directions, as schematically represented in Figure 2. Four different types of GFRP laminates are considered: Type A - *chopped strand material* (CSM) with discontinuous fibres randomly disposed, resulting in a laminate thickness of 2.5 mm; Type B - fibres oriented at ±45º and thickness of 2.5 mm; Type C - 80 % of fibres oriented at ±45º, 10 % oriented at 0º and 10 % oriented at 90º, with thickness of 2.5 mm; Type D - 80 % of fibres oriented at ±45º, 10 % oriented at 0º and 10 % oriented at 90º, with thickness of 5 mm. The minimum content of polyester resin is used to guarantee the fibres impregnation.

Type A:
5 layers CSM (450 g/m²)

Type B:
8 layers ±45º (400 g/m²)

Type C:
6 layers ±45º (400 g/m²)
1 layer 0º/90º (600 g/m²)

Type D:
12 layers ±45º (400 g/m²)
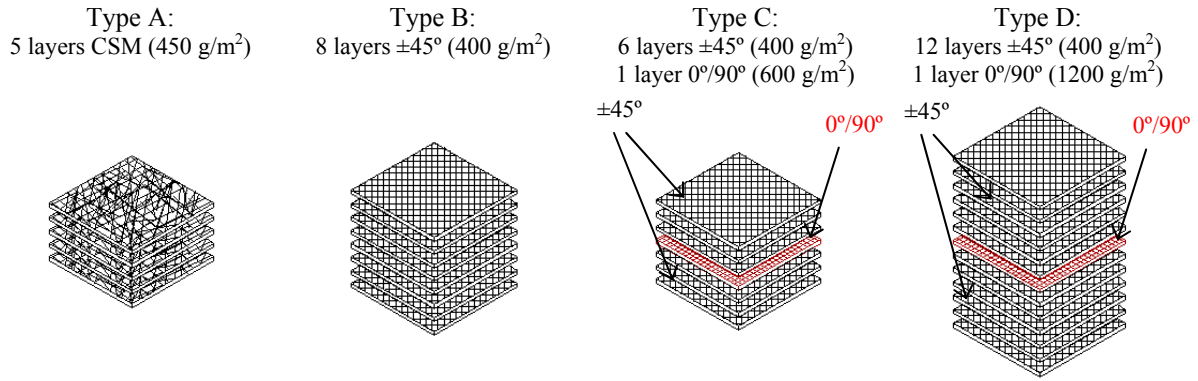1 layer 0º/90º (1200 g/m²)

Figure 2: Schematic representation of investigated laminates.

The total quantity of fibres disposed in each direction of the laminates is presented on Table 1.

Table 1: Characteristics of fibre reinforcement configurations for the three types of tested laminates.

Reference	Thickness – e [mm]	Reinforcement	0º	90º	+45º [g/m²]	-45º
Type A	2.5	CSM		2250		
Type B	2.5	100% ± 45º	-	-	1600	1600
Type C	2.5	80% ± 45º + 10% 0º + 10% 90º	300	300	1200	1200
Type D	5.0	80% ± 45º + 10% 0º + 10% 90º	590	610	2400	2400

The GFRP specimens are produced at PIEP - Institute for Innovation in Polymer Engineering facilities, using the technique of *Vacuum Assisted Resin Transfer Moulding* – VARTM. This technique consists in overlapping layers of dry glass fibre inside a closed and sealed mould, and then injecting resin with lower pressure by vacuum (see Figure 3a). After the process of cure, the samples are cut (Figure 3b) and perforated (Figure 3c).
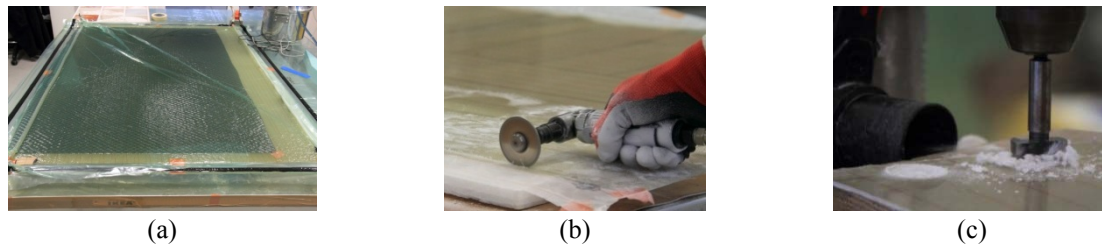

(a)   (b)   (c)

Figure 3: Production of specimens: (a) resin injection; (b) cutting; (c) drilling.

The tested samples consist on flat, constant rectangular cross-section specimens with a centreline hole located near the end of the specimen. The geometry of specimens is the same of the PERFOFRP connectors investigated in a previous work [1]. They are conceived to be representative of the two main failure modes verified on the previously conducted pull-out tests: a) bottom failure that occurs below the hole and b) lateral failure that occurs between two holes. The specimen's geometry for each type of failure mode is represented in Figure 4a and Figure 4b, respectively. The number of specimens tested for each geometric and material configuration is listed in Figure 4c.
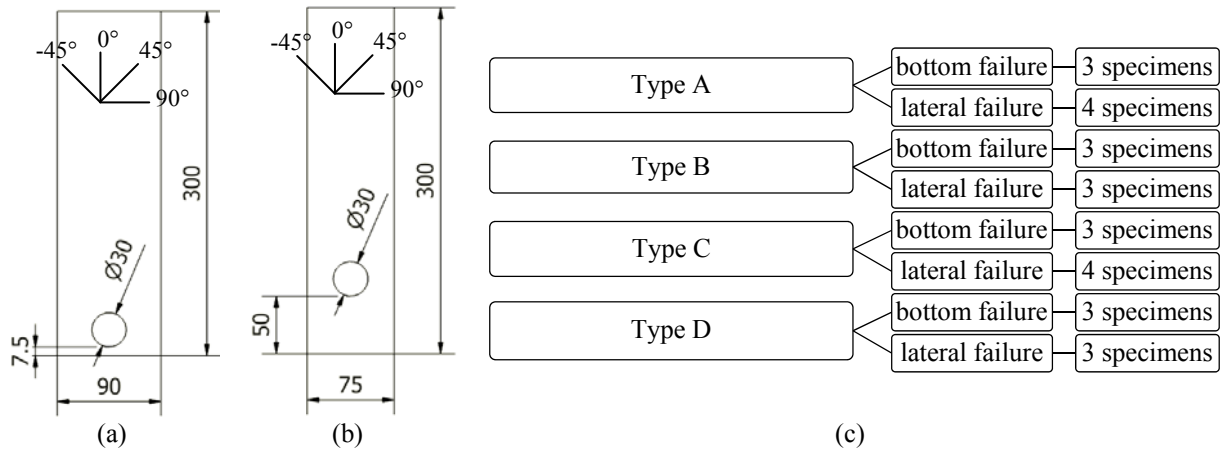
Figure 4: Test specimens: a) specimen designed for bottom failure; b) specimen designed for lateral failure; c) number of specimens tested for each material and geometric configuration (units in mm).

3. MECHANICAL PROPERTIES OF LAMINATES

Direct tensile tests are performed on representative samples with 250 mm length and 25 mm width to evaluate the behaviour of the different laminates. These tests are carried out following the procedures described on the ASTM D3039 [9]. A clip-gauge of 50 mm of reference length (Figure 5a) is applied at mid height of each sample to determine the longitudinal deformation of the specimens. The stress-strain relationships obtained are presented in Figure 5b. The average values of maximum tensile stress, maximum strain and modulus of elasticity obtained from tensile tests are presented in Table 2.
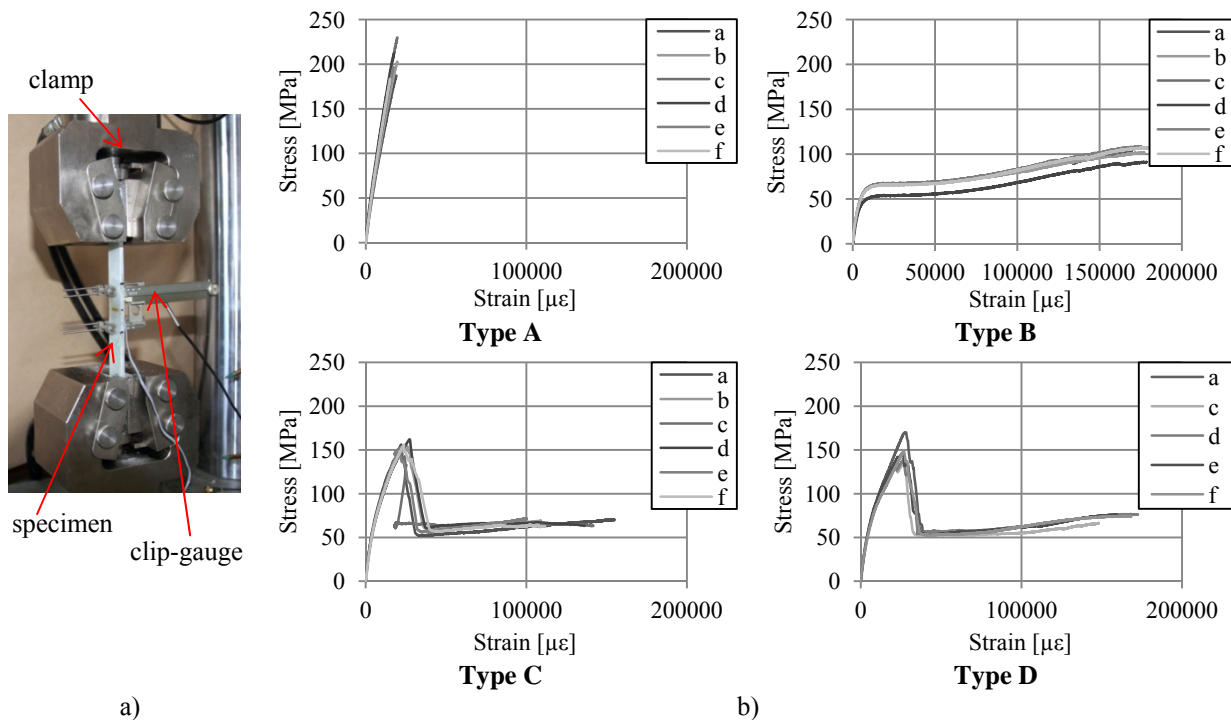

Figure 5: Direct tensile tests with GFRP laminates: a) test setup; b) stress-strain relationship (direction 0°).

As shown in Figure 5, the GFRP Type A presents the more fragile rupture between the studied laminates. This GFRP also presented the lower ultimate strain along the direction 0°. These results are expectable since the laminate Type A is comprised of short fibres. On the other hand, the GFRP Types C and D presented a peak at about 30000 $\mu\varepsilon$ and kept a residual strength corresponding to nearly 30% of the tensile strength. In these laminates the peak occurs due the rupture of the fibres oriented in the load direction

4

(0°), and the residual strength is provided by the high content of fibres on the (±45°). The laminate type B presented the common response for this kind of FRP, showing a hardening behaviour until the ultimate strain, without a peak.

Table 2: Results from tensile tests (direction 0°).

| Reference | Tensile strength | | Ultimate Strain | | Modulus of elasticity | |
	Average [MPa]	Coef. of Variation [%]	Average [με]	Coef. of Variation [%]	Average [GPa]	Coef. of Variation [%]
Type A	202.03	7.78	18044.35	9.91	11.98	7.36
Type B	102.90	5.73	176345.35	9.36	13.20	10.68
Type C	154.63	2.71	125638.84	7.92	8.84	5.22
Type D	146.78	7.74	141972.95	2.27	8.98	4.47

4. TEST PROCEDURES AND INSTRUMENTATION

The test is carried out by pulling the specimen in tension with a clamp. Rectangular steel plates are attached on top of all specimens in order to provide an appropriate anchorage during testing and better distribute the tensile forces induced by the clamp. At bottom the specimen is inserted in the groove of a steel cylinder device and crossed by a close tolerance aluminium pin positioned in the hole of the specimen. The groove of the steel cylinder where the specimen is positioned is large enough to avoid out-of-plane contact of the specimen with the groove walls. This configuration applies a bearing load to the bottom part of the specimen, as represented in Figure 6, where the full test setup is shown.
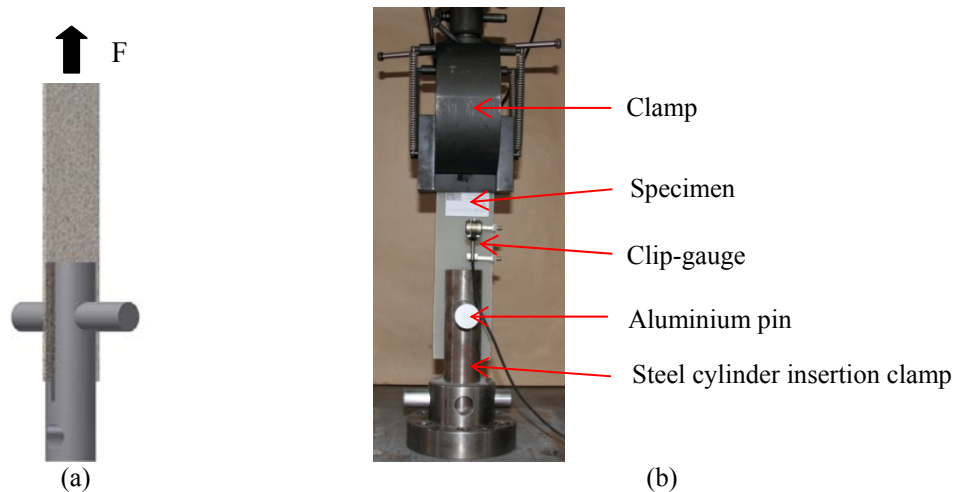

(a)   (b)

Figure 6: Test setup: a) loading scheme; b) clamps, supports and instrumentation.

The aluminium pin simulates the presence of the concrete dowel that is formed when the connector PERFOFRP is embedded in a concrete slab. The most appropriate element to simulate the concrete dowel formed in a sandwich panel with perforated connectors would be a concrete pin. However, the concrete pin is difficult to obtain and it is fragile. In this case, the pin could suffer failure before the GFRP connector, which is not intended. The aluminium pin is chosen because its tensile and compressive strength are superior to those of concrete, and its modulus of elasticity, although higher than concrete's modulus of elasticity (approximately the double), is significantly lower than that of steel. Thus, the aluminium pin guarantees that the failure occurs on the GFRP specimen and not at the pin.

During testing, the tensile load is applied to the GFRP specimen with a constant displacement rate of the piston of the actuator of 2 mm/min. A load cell with a capacity of 200 kN registers the load applied to the specimen. An exemplar of each type of specimen tested is instrumented with strain gauges (SG). The SG is bonded to the specimen where the failure is expected to occur. Two SG are placed in specimen's with lateral failure, one in front and the other on the back of the specimen, as represented in Figure 7a. Only one SG is placed just below the hole in the specimen with bottom failure, as shown

in Figure 7b. A clip-gauge with 50 mm of reference length is positioned at each sample's middle height to determine the longitudinal deformations (Figure 7c).
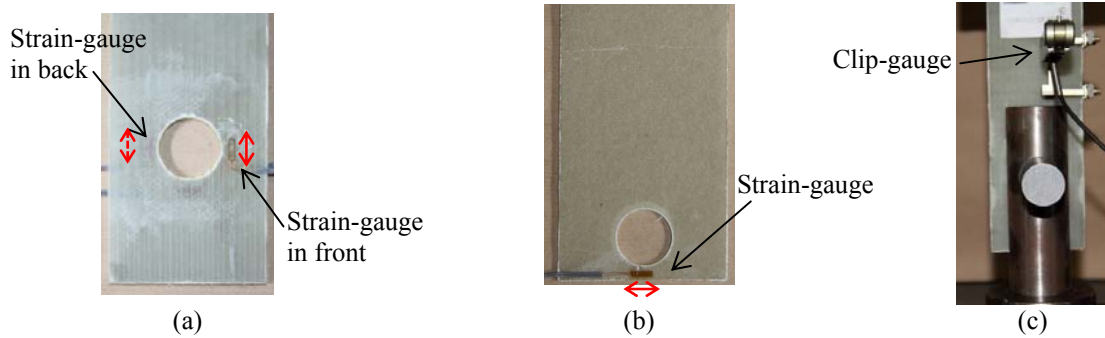

| (a) | (b) | (c) |

Figure 7: Specimens' instrumentation: a) SG in a specimen with lateral failure; b) SG in a specimen with bottom failure; c) clip-gauge.

5. EXPERIMENTAL RESULTS

5.1 Failure modes

After testing, all the specimens are observed and it is possible to verify that, in almost all situations, the experimental failure modes match the expected ones. The failure modes observed in the specimens are indicated in Figure 8.
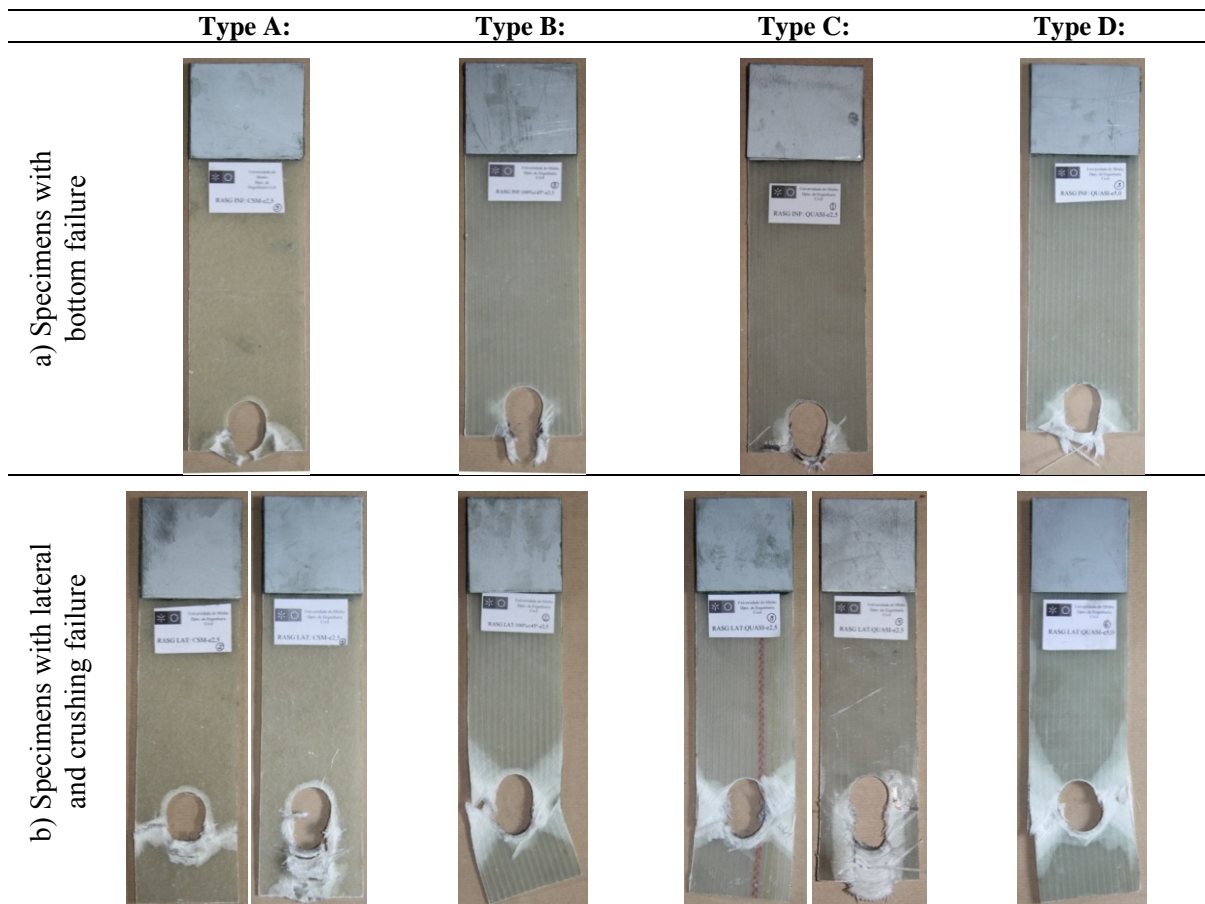

Figure 8: Failure modes

The failure mode is similar in all specimens designed to provide bottom failure. In fact, in all the specimens with this configuration, the damage starts at the smaller dimension below the hole, followed

by the formation of inclined cracks towards the hole. In specimens designed for lateral failure, the damage is predominantly concentrated in the lateral area of the hole. Crushing is also verified in the lower zone of hole. Crushing in the lower zone of the hole, without lateral failure, has occurred in specimens of Type A and Type C. In specimens of Type B, C and D, the lateral failure is more ductile and covers a greater area on the lateral zone of the hole. In specimens of Type A, the damage is more localized due to the smallest effective fibre content bridging the critical failure plane. Particularly, in specimens of Type B, C and D, the lateral failure occurs in a gradual manner, revealing the stress redistribution capacity provided by the relatively high content of fibres in these specimens. Particularly in the specimens with long fibres oriented in the 45°, the first crack generally appears in the GFRP located in one of the lateral sides of the hole, causing the rotation of the specimen. However, the tests are symmetric up to a relatively high level of damage.

5.2 Load capacity and load *vs.* displacement behaviour
Table 3 presents the results of average maximum load attained in the various tested specimens. The average load values are obtained from 3 or 4 similar specimens, as reported in Figure 4c.

<div align="center">

Table 3: Average maximum load

Failure mode	Reference	Thickness - e [mm]	Average load [kN]	Coef. ofvariation [%]
a) Specimens with bottom failure mode	Type A	2.5	9.78	18.02
	Type B	2.5	11.09	3.23
	Type C	2.5	12.29	6.16
	Type D	5.0	26.27	4.49
b) Specimens with lateral and crushing failure mode	Type A	2.5	6.53	4.16
	Type B	2.5	6.29	0.98
	Type C	2.5	6.25	7.39
	Type D	5.0	13.00	2.08

</div>

Figure 9 compares the load versus displacement curve for representative types of specimens. The behaviour of the specimens of the same type is similar. The displacement corresponds to the internal displacement of the actuator and not the specimens' deformation.
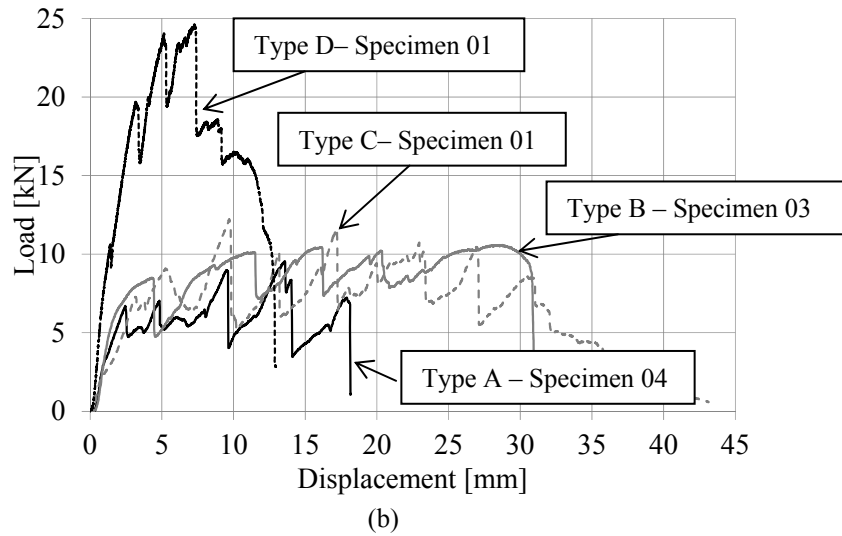

(a)

(b)
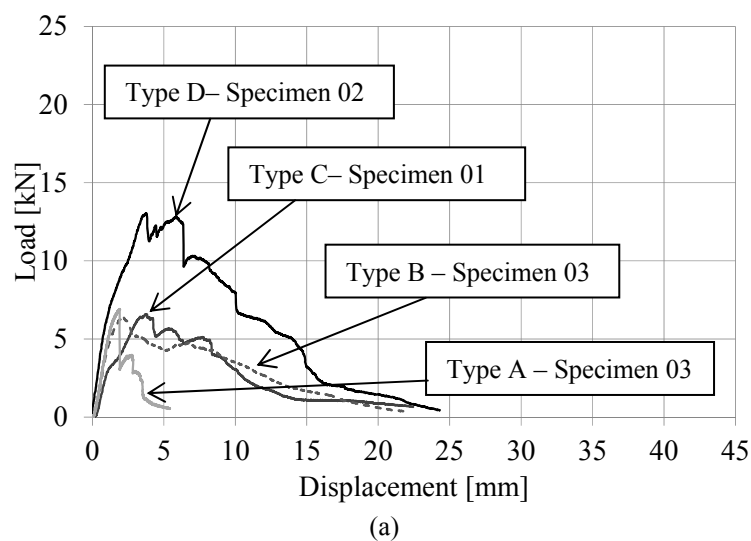
Figure 9: Load *vs.* displacement curves obtained for specimens with: a) bottom failure mode;
b) lateral failure mode.

The behaviour is more fragile in specimens of Type A, designed for bottom failure, than in other types. This fragile behaviour is characterized by a sudden loss of load that occurs after the maximum load is reached. In addition, the deformation capacity of this type of laminate is lower than the one registered in the other types of specimens. Still regarding the bottom failure mode, the behaviour of specimens of Type B and C is very similar in terms of maximum load and deformation capacity. These specimens present higher deformation capacity than specimens of Type A.

The behaviour of all samples with lateral failure mode and thickness of 2.5 mm is similar. After the maximum load is attained, the behaviour for these specimens is characterized by several load drops, followed by recoveries. This process is repeated until the final rupture of each tested specimen, which occurred at relatively high displacement, much higher than the failure displacement in specimens designed for bottom failure. Regarding the specimens of Type D with lateral failure mode, despite the higher loading capacity, the rupture is more fragile.

Figure 11 compares stress versus strain diagrams recorded from the SG applied in the vicinity of hole for representative types of specimens. The tensile stress value is determined for the regions of the laminate located in the lateral of the hole, assuming a uniform stress distribution in this region (Figure 10):

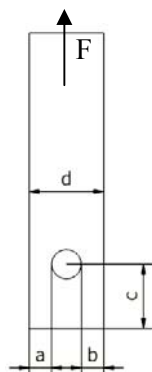$$Tensile\ stress = \frac{F}{(a+b) \times e} \tag{1}$$

Figure 10: Generic dimensions of the test specimens (F is the load registered by the load cell and e is the nominal thickness of the laminate).

During the tests, some strain gauges became damaged, due to early failure of the specimen in the zone where the SG is glued. The curves presented in Figure 11 only show valid SG results (until the specimen failure).

In specimens designed for lateral failure, two SG are placed on opposite sides, and the results obtained from both of them are very similar. This means that the evolution of strains on both sides of the hole is similar, proving that the behaviour of specimens is symmetric up to a relatively high level of damage. In Figure 11b, the strain values correspond to the average of the strains recorded in the two SG.

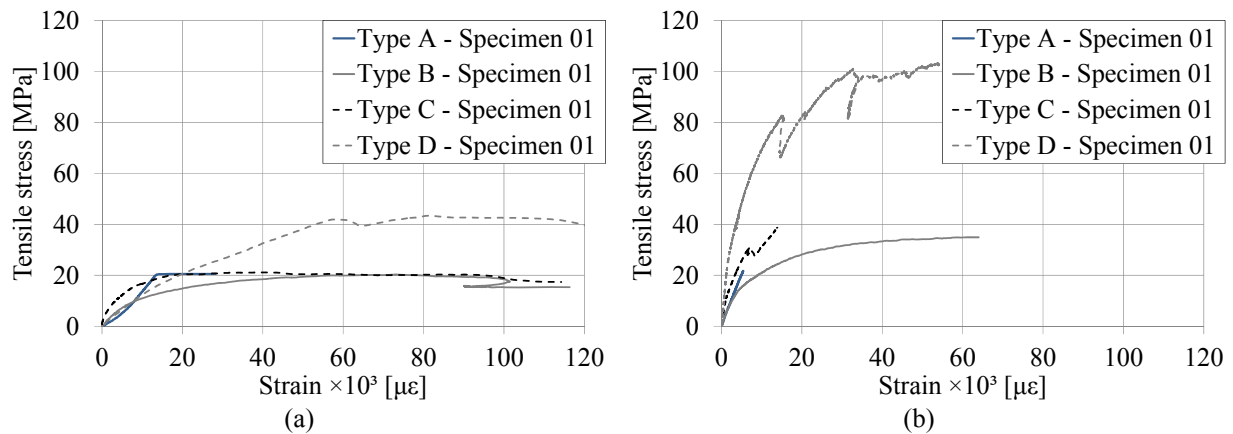In general, the strains measured in all the specimens are very small.

Figure 11: Typical tensile stress-strain diagrams in the vicinity of the hole: a) specimens with bottom failure mode; b) specimens with lateral failure mode.

6. CONCLUSIONS

The present paper describes an experimental study carried out to characterize the failure modes associated with GFRP perforated connectors used in concrete sandwich panels. The study includes an experimental program for the characterization of the tensile behaviour of different GFRP laminates, and an experimental program with GFRP perforated rectangular specimens. This last program is performed to analyse the specimens' failure modes, as well as load and deformation capacity. The obtained results evidence the influence of the percentage and arrangement of the fibres on the tested GFRP specimens in terms of failure mode, load and deformation capacity. The results show that for the same type of specimen and the same thickness, the maximum load values are similar, regardless the fibres orientation.

By increasing the thicknesses of the specimen, a proportional increase in maximum load is observed. In all types of GFRP specimens, it is verified that the maximum load values associated with lateral failure are higher than the maximum load values registered in specimens with failure bellow the hole.

REFERENCES
[1] R.M. Lameiras, I. Valente, J. Barros, M. Azenha, P. Ferreira, Fibre reinforced polymer (FRP) connectors for steel fibre reinforced self-compacting concrete (SFRSCC) sandwich panels, in: 6th International Conference on FRP Composites in Civil Engineering (CICE 2012), Rome, 2012.

[2] R.M. Lameiras, J. Barros, M. Azenha, I. Valente, Sandwich structural panels comprising thin-walled Steel Fibre Reinforced Self-Compacting Concrete (SFRSCC) and Fibre Reinforced Polymer (FRP) connectors, in: 8th RILEM International Symposium on Fibre Reinforced Concrete (BEFIB 2012), Guimarães, Portugal, 2012.

[3] R. Lameiras, C. Gonçalves, I. Valente, J. Barros, M. Azenha, Caracterização ao corte da ligação entre conector de GFRP e betão auto-compactável reforçado com fibras de aço (in Portuguese), in: FEUP (Ed.) BE2012 - Encontro Nacional Betão Estrutural 2012, Porto, Portugal., 2012.

[4] I. Valente, Experimental Studies on ShearConnectionSystems inSteelandLightweight Concrete Composite Bridges, PhD Thesis Thesis, Civil Engineering Department – School of Engineering, University of Minho, 2007.

[5] E.C. Oguejiofor, M.U. Hosain, A parametric study of perfobond rib shear connectors, Canadian Journal of Civil Engineering, vol. 21 (1994) 614-625.

[6] G.S. Veríssimo, Desenvolvimento de um conector de cisalhamento em chapa dentada para estruturas mistas de aço e concreto e estudo do seu comportamento, PhD Thesis Thesis, PhD Thesis, Universidade Federal de Minas Gerais, Belo Horizonte., 2007.

[7] E.C. Oguejiofor, M.U. Hosain, Numerical analysis of push-out specimens with Perfobond rib connectors, Computers & Structures, vol. 62 (1996) 617-624.

[8] R. Lameiras, T. Santos, J. Barros, M. Azenha, I. Valente, Desenvolvimento de painéis sandwich estruturais constituídos por camadas nervuradas de betão auto-compactável reforçado com fibras de aço e conectores de compósito polimérico reforçado com fibras de vidro" (in Portuguese), in: BE2012 - Encontro Nacional Betão Estrutural 2012, FEUP, Porto, Portugal., 2012.

[9] ASTM Standard D 3039/D 3039M, Tensile Properties of Polymer Matrix Composite Materials, ASTM International, 2008.